Functionally graded NiTi shape memory alloys

F.E. Ferreira[a, *], A.R. Alves[a], J.P. Oliveira[a], F.M. Braz Fernandes[a]

[a]CENIMAT – Centro de Investigação de Materiais, Faculdade de Ciências e Tecnologia – Universidade Nova de Lisboa, Campus de Caparica,
2829-516 Caparica, Portugal

Abstract

In this study, in order to obtain a functionally graded material, NiTi strips were annealed at 350°C, 450°C and 550°C in a furnace using an assembly that allowed a temperature gradient along them, and their transformation temperatures were studied by Differential Scanning Calorimetry (DSC). Furthermore, the strips were bent at both ends and dipped into a water bath at room temperature which was then heated to 61°C in order to observe the influence of the gradient annealing on their strain recovery. It was found that the strips' coolest regions presented the greatest strain recovery, particularly the strips annealed at 350°C and 450°C, although any strip exhibited a full strain recovery, due to plastic deformation during bending. These results, together with the DSC analysis at both regions (coolest and hottest), allow us to conclude that the graded annealing was successful for the intended functional gradient, as a gradient of transformation temperatures along the strips has been obtained, despite the primitive assembly, thus presenting an interesting result for a first approach. Further tests will be performed with a new experimental procedure especially designed for this purpose.

1. Introduction

Shape memory alloys are unique materials with the ability to produce large recoverable deformations and perform mechanical work when undergoing a temperature or stress variation. Among them, near-equiatomic NiTi alloys have a prominent place due to their transformation-based actuation mechanism with high strain recovery (up to 8%), high stress generation (up to 900 MPa) and high specific actuation energy density (up to thousands of J/kg), and their capability to perform more than 10^5 actuation cycles [1,2]. These properties together with their high mechanical strength and biocompatibility [3] allow the simplification, miniaturization and cost reduction of multiple actuation and control devices in engineering applications (flow-restricting thermostats, refrigerant expansion valves [1], morphing structures like aircraft wings and inlets [4-6], orthodontic wire, guide wire, stents [7], and many others), replacing complex and bulky electromechanical and hydraulic systems.

However, the low temperature range of thermally induced martensitic transformation and the superelastic deformation behaviour that NiTi alloys exhibit during stress induced transformation make these alloys to perform a full transformation when a threshold value of stress or temperature is reached, rendering difficult a progressive control of displacement [8-10]. To overcome this limitation and improve NiTi actuators controllability, martensitic transformation temperature and critical stress have to vary along the material. Due to the high ageing sensitivity of Ni-rich NiTi alloys [1], a gradient age-annealing along them must provide a microstructural gradient along the material and so an almost continuous variation of martensitic transformation temperature and stress, thus creating functionally graded NiTi [8,11,12]. Besides, some authors have also created functionally graded NiTi by laser surface

---

* Corresponding author.

E-mail address: fe.ferreira@campus.fct.unl.pt (F.E. Ferreira)

anneal [13], geometry variations [14] and electrical resistance heating [15].

2. Experimental

Commercial NiTi (Ti-51 at.% Ni) alloy (ribbon 0.9x 0.3 mm, from *Memory-Metalle GmbH)*, with about 10 cm long, henceforward denoted by AR ("as-received"), were heat treated at 450°C for 1.8 ks (denoted as sample Ref) and quenched in water. Then, to achieve the temperature gradient, the strips were inserted in a ceramic block up to half of their length (5 cm), and annealed at 350°C (sample I), 450°C (sample II) and 550°C (sample III) for 1.8 ks in a furnace, and quenched in water. To reach the greatest temperature gradient possible, the ceramic block was placed at the centre of the furnace with the strips aimed to its centre as outlined in Fig. 1, and a thermocouple was positioned near the ceramic block for temperature control inside the furnace (the temperature indicated for the gradient heat treatment is the temperature measured at the higher temperature region ("H" in Fig. 1). The temperature inside the ceramic block was not collected; however, it was significantly lower than the outside of it. Samples were collected from the annealed strips ("hot" and "cold" regions) for differential scanning calorimetry (DSC). *DSC 204 F1 Phoenix* model from *Netzsch* was used to ascertain about the transformation temperatures and the temperatures. DSC analysis was also carried out in AR strips for comparison. Beyond that, annealed strips were then bent at both ends and placed on a water bath at room temperature, which was then heated to 61°C in order to observe the influence of the annealing gradient in their strain recovery.
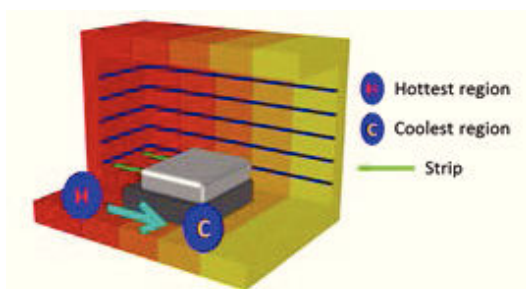

Fig. 1. Schematic of the strips inserted in a ceramic block in the furnace.

3. Results and Discussion

3.1. DSC analysis

Figs. 2 and 3 show the DSC curves of the strip annealed at 450°C for 1.8 ks without any gradient and the ones gradient annealed at 350°C, 450°C and 550°C for the regions inside the ceramic block (region "C") and outside the ceramic block (region "H"), respectively. All transformation temperatures are summarized at Table 1. Transformation temperatures were collected for 1% and 99% of transformation via a transformation kinetics model. Some transformation temperatures could not be collected because of transformation overlapping or, in case of martensitic finish temperatures, because these were below -150°C.
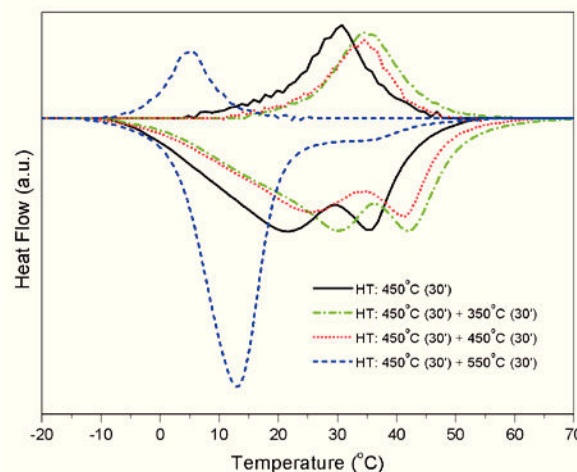

Fig. 2. Results of the DSC analysis for the strips portions inside the ceramic block (region "C").
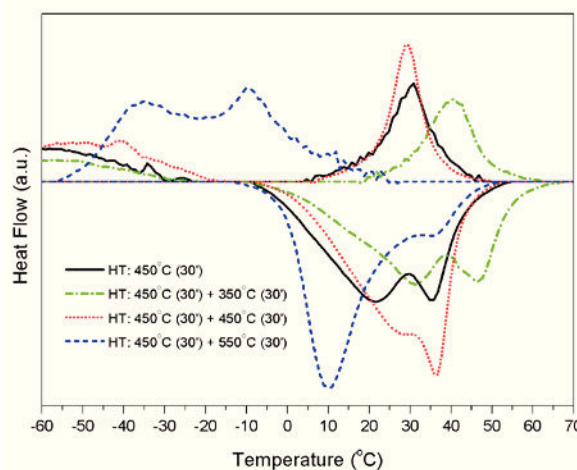

Fig. 3. Results of the DSC analysis for the strips portions outside the ceramic block (region "H").

Table 1. Transformation temperatures for all heat treatments.

		Sample						
		Ref	I-C	II-C	III-C	I-H	II-H	III-H
Cooling	R_s	43.8	52.2	46.7	18.7	56.7	43.8	18.8
	R_p	28.8	34.7	32.7	4.7	38.7	27.8	-9
	R_f	7.8	17.7	14.2	-6.3	20.7	10.8	-15
	M_s	-32.2	-31.3	-29.8	-32.3	-31.3	-23.2	-
	M_p	-	-	-	-48.8	-	-	-34.9
	M_f	-	-	-	-67.3	-	-	-51.2
Heating	R_s	-3.2	-1.8	-4.3	-5.8	-1.3	-0.2	-5.2
	R_p	21.7	30.2	25.2	-	31.2	28.7	-
	R_f	-	-	-	-	-	-	-
	A_s	-	-	-	-	-	-	-
	A_p	35.7	41.7	41.2	-	-	-	-
	A_f	46.8	58.7	54.2	44.7	57.7	45.8	43.8

The AR strip did not experience any phase transformation revealing that it was work-hardened, and it is not represented. However, after the first annealing at 450°C for 1.8 ks, recrystallization has occurred and the martensitic transformation was observed. It can also be noticed that both direct and inverse transformations occur in two-steps (austenite↔R-phase↔martensite). Moreover, the transformation temperatures decreased with increased annealing temperature and, at room temperature, the strip tips from gradient annealing I and II exhibited martensite, R-phase and some residual austenite, while strip tips from annealing III were almost fully austenitic and with some residual R-phase and/or martensite that, according to DSC analysis, is fully transformed at 50°C. The variation of some transformation temperatures for each sample can be depicted in Fig. 4. The temperatures chosen for representation are the ones involved in shape memory effect. Denominations "C" and "H" for the samples I, II and III refer to the region where the samples were collected.
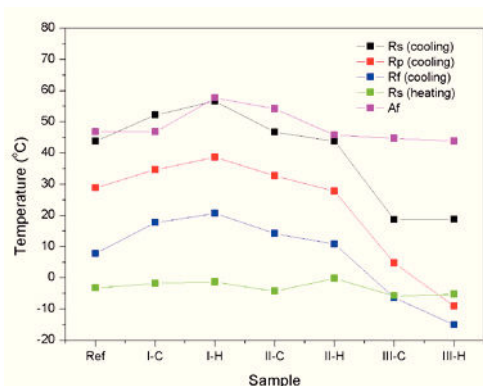

Fig. 4. Variation of some transformation temperatures for each sample.

3.2. Strain recovery

Fig. 5 presents a scheme of the strain recovery of the strips during heating in a water bath from room temperature to 61°C. It can be observed that for annealing I and II between 48.1°C and 58°C occurs a great strain recovery at both regions ("H" and "C"). This is consistent with the results from the DSC analysis, where it is noticed that, at those temperatures, reverse transformation is almost complete (Figs. 2 and 3). However, austenite is fully transformed at about 60°C for region "C" strip tips. Fig. 5 also shows that strip portions inside the ceramic block (region "C") annealed at 350°C and 550°C had a greater strain recovery of their original shape at all temperature stages, comparing with region "H" portions, and for annealing at 450°C the portions from region "H" had a greater strain recovery at all temperature stages. These results are also consistent with the DSC analysis that shows that austenitic finish temperature for annealing at 350°C and 550°C are lower at region "C" and for annealing at 450°C is lower at region "H" (Fig. 4). Furthermore, as depicted, do not take place a complete strain recovery in any strip, suggesting that plastic deformation occurred during the strips bending. That might also be the justification for the lower strain recovery of strip portions with the lower austenitic finish temperature, since, as known, any deformation at the austenitic phase beyond the superelastic limit gives rise to the presence of plastic and thus irrecoverable deformation.
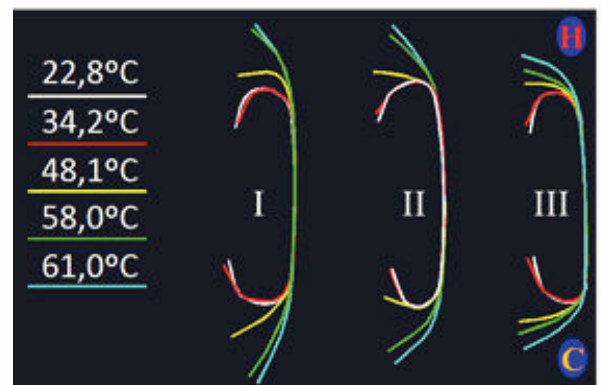

Fig. 5. Scheme of the gradient annealed strips at different temperatures after bending.

4. Conclusions

The following conclusions can be drawn from this work:

− The functional gradient caused by the different annealing temperatures along the strips has been

clearly put in evidence, despite the simplicity of the experimental assembly;

− It was observed that increased annealing temperature decreased the austenitic finish temperature for annealing at 450°C and 550°C and increased for 350°C;

− Further tests are currently in progress with a new experimental procedure especially designed for this purpose, where a controlled temperature can be applied on a given region of the material performing the heat treatments on selected regions. Thus, it will be possible to control the transformation temperatures along different regions of the material as desired.

Acknowledgements

References

[1] K. Otsuka, X. Ren, Prog. Mater. Sci. 50 (2005) 511.
[2] W. Huang, Mater. Des. 23 (2002) 11.
[3] D.C. Lagoudas, Shape Memory Alloys: Modeling and Engineering Applications. Springer, 2008.
[4] A. Guion, C. Hanna, P. Hutapea, Jinho Kim, N. Heulitt, Aircr. Eng. 80 (2008) 839.
[5] D.C. Lagoudas, D. Harti, Aerospace Engineering Department, Texas A & M University, 2007.
[6] K.T. Tan, W.K. Yeo, A.Y.N. Soa, S.A. Meguid, Mater. Des. 31 (2010) 1284.
[7] Johnsons Medical. Nitinol - Shape Memory <http://jmmedical.com/nitinol/27072/Shape-Memory.html>, 2015 (accessed 29.06.2015).
[8] A. Mahmud, Y. Liu, T. Nam, Smart Mater. Struct. 17 (2008) 1.
[9] J. A. Shaw, S. Kyriakides, J. Mech. Phys. Solids 43 (1995) 1243.
[10] G. Tan, Y. Liu, P. Sittner, M. Saunders, Scr. Mater. 50 (2004) 193.
[11] M.F. Razali, A.S. Mahmud, J. Alloys Compd. 618 (2015) 182.
[12] A.S. Mahamud, Y. Liu, T.H. Nam, Phys. Scr. (2007) 222.
[13] Q. Meng, Y. Liu, H. Yang, B.S. Shariat, T. Nam, Acta Mater. 60 (2012) 1658.
[14] B.S. Shariat, Y. Liu, G. Rio, Mater. Des. 50 (2013) 879.
[15] Q. Meng, H. Yang, Y. Liu, T. Nam, D. Favier, J. Alloys Compd. 577 (2013) S245.